ditional error of 0.017 to $\alpha(0)$.

[11]V. Barger, in *Proceedings of the Seventeenth International Conference on High Energy Physics, London, England, 1974*, edited by J. R. Smith (Rutherford High Energy Laboratory, Didcot, Berkshire, England, 1975), p. I-193.

High-Statistics Study of ω^0 Production*

M. H. Shaevitz,† N. W. Reay, K. Reibel, and N. R. Stanton
Physics Department, The Ohio State University, Columbus, Ohio 43210

and

K. W. Edwards and G. Luxton‡
Department of Physics, Carleton University, Ottawa, Ontario K1S 5B6, Canada

and

M. A. Abolins and R. A. Sidwell
Physics Department, Michigan State University, East Lansing, Michigan 48823

and

J. A. Dankowych, G. J. Luste, J. F. Martin, and J. D. Prentice
Department of Physics, University of Toronto, Toronto, Ontario M5S 1A7, Canada
(Received 29 October 1975)

We report results from a study of $\pi^- p \to \omega^0 n$ at 6.0 GeV/c based on 28 000 events from a charged and neutral spectrometer. Background under the ω^0 is only 7%, a large improvement over deuterium–bubble-chamber work. Density matrix elements, projected cross sections, and effective trajectories for natural and unnatural exchanges are presented.

Previous work[1-8] on $\pi N \to \omega N$ has been limited by the difficulties of dealing with neutral particles in the final state, and the best data have so far come from deuterium–bubble-chamber experiments. We report here the results of a study of $\pi^- p \to \omega^0 n$ at 6.0 GeV/c using a charged and neutral spectrometer at the Argonne National Laboratory zero-gradient synchrotron. Our sample of 28 000 $\omega^0 n$ events is 8 times larger than that of any previous ωN experiment.

The apparatus, described elsewhere,[9,10] combines a large-aperture magnetic spectrometer with a γ detector employing spark chambers and a lead-glass Cherenkov array. The vector momenta of both charged pions and both γ's from $\omega \to \pi^+\pi^-\pi^0$ are measured; the neutron is unseen.

Histograms of $\pi^+\pi^-\pi^0$ effective mass, and of nucleon missing mass recoiling against the ω^0, are shown for three intervals of $t' = t - t_{\min}$ in Figs. 1(a)–1(f). There is no dependence of the positions or widths of the η, ω, or neutron peaks on t'. The cuts which define ω and neutron events are indicated by vertical lines; control regions BG in Figs. 1(a)–1(c) are used for background subtraction. Background under the ω averages 6.6%, and is 9.8% for $|t| < 0.05$ (GeV/c)^2. This is a significant improvement over deuterium–bubble-chamber experiments, where backgrounds typically[1,4] average more than 30% and are considerably worse at small t'. A correction of (7 ± 1)% has been applied for ω's outside the mass cut (in addition to the 10% for unseen decay modes[11]). The corrected ω yield is stable against reasonable changes in the width and location of the control regions.

A rather tight cut (0.5 to 1.1 GeV/c^2) has been made on the nucleon mass to reduce further the small contamination of $\omega^0\Delta^0$ which is not rejected by veto counters[9] surrounding the target; a correction of (13 ± 2)% was applied for good neutrons rejected by this cut. The remaining $\omega\Delta$ contamination [(3.8 ± 0.5)%] has been estimated and removed by examining events for which one target veto counter fired, and also by fitting the departure of the neutron peak from a symmetric shape. Since ω events with nucleon missing mass 1.1–1.3 GeV/c^2 are found to have density matrix elements and t' distributions very similar to those inside the neutron cut we are confident that the effects of $\omega\Delta$ contamination in our data are negligible.

A large change in t' dependence of the back-

ground occurs for events with $\pi^+\pi^-\pi^0$ mass $M_{3\pi}$ just above the ω, from a forward turnover at $M_{3\pi} = 0.8$ GeV/c^2 to a sharp forward peak by $M_{3\pi} = 0.9$ GeV/c^2. It is important to understand the origin of these very peripheral events, most of which have $|t'| < 0.05$ (GeV/c)^2, because our background subtraction is based in part on the control region $0.845 < M_{3\pi} < 0.890$ GeV/c^2. We find that most of these events have the mass of the negatively charged di-pion $M_{\pi^-\pi^0}$ in the ρ region.[12] Thus the peripheral events are probably associated $\rho^- N^{*+}$ production, possibly produced via pion exchange,[13] and should not be subtracted as background under the ω. We have excluded them by the cut $M_{\pi^-\pi^0} < 0.6$ GeV/c^2 applied to both signal and background; this cut was used in the spectra shown in Figs. 1(a)–1(c). Its effect for $|t'| < 0.05$ (GeV/c)^2 is shown in Fig. 1(g), where the shaded events are those removed by the cut. We emphasize that the effect on the ω peak is always negligible, and that the effect on the background is negligible for $|t'| > 0.08$ (GeV/c)^2. (The penalty for *not* making this di-pion cut is as follows: The forward peaking of the density matrix element ρ_{00} is increased even more, by 20% in the most forward bin of t'; the turnovers in $d\sigma/dt$ and $\rho_+ d\sigma/dt$ become even more pronounced; but $\rho_{00} d\sigma/dt$ remains nearly unchanged.)

The method of moments was used to extract the density matrix elements from the angular distribution $f(\cos\theta, \varphi)$ of the normal to the decay plane in the s-channel helicity frame. A Monte Carlo program simulated the acceptance limitations of experimental geometry, interaction and decay of final-state particles, and cuts on the π^0-decay asymmetry and minimum shower energy. Both the data and the several million Monte Carlo events were binned in a 40× 36 grid of $\cos\theta, \varphi$; events in the BG control regions were subtracted in each bin. The Monte Carlo acceptances used to weight the data showed a maximum variation (as a function of $\cos\theta$ and φ) of a factor 3 at a given t'.

The moments of the spherical harmonics $Y_M^L(\cos\theta, \varphi)$, obtained with the same method, test our understanding of the experimental acceptance: Imaginary parts of Y_M^L's should be zero, and Y_M^L's with $L > 2$ are expected to be small. We find that these "illegal" moments are very small in the ω^0 region, with the largest contributing 2% of the cross section. An additional check is available from the ω Dalitz-plot density, where a linear population of events is expected in $R_D = |\vec{p}_+ \times \vec{p}_-| / |(\vec{p}_+ \times \vec{p}_-)_{max}|$ for the simplest decay matrix

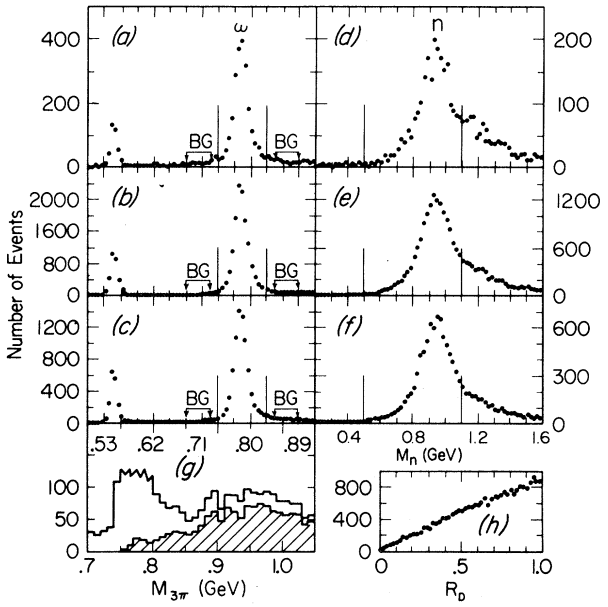

FIG. 1. (a)–(c) $\pi^+\pi^-\pi^0$ effective mass for $|t'|$ intervals 0.0–0.05, 0.05–0.30, and 0.30–1.20 (GeV/c)^2, respectively. (d)–(f) Nucleon missing mass for ω events in the same $|t'|$ intervals. (g) Effect of the di-pion mass cut on the $\pi^+\pi^-\pi^0$ spectrum for $|t'| < 0.05$ (GeV/c)^2. The shaded events are removed by the cut. (h) Radial Dalitz-plot density for events in the ω region.

element; here $\vec{p}_+$ and $\vec{p}_-$ are the π^+ and π^- momenta in the ω center-of-mass frame. Figure 1(h) demonstrates that our data satisfy this linear relation quite well even before the acceptance correction is made.

It has been predicted[14-16] that $\rho\omega$ interference effects could lead to a sizable difference in the projected cross sections $\rho_{00} d\sigma/dt$ at small t' for the charge-symmetric reactions $\pi^- p \to \omega n$ and $\pi^+ n \to \omega p$. We are presently measuring this effect by collecting data on both reactions in deuterium. Very preliminary results indicate that $\rho_{00} d\sigma/dt$ for the $\pi^+ n$ reaction is roughly 20% above that for $\pi^- p$ for $|t'| < 0.1$ (GeV/c)^2; this difference must be kept in mind when comparing our data with those from $\pi^+ n$ experiments.

Our results are presented in Fig. 2. The error flags do not include an overall normalization uncertainty of ±8%. Density matrix elements ρ_{ij} in the s-channel helicity frame are shown in Figs. 2(a)–2(d), and the corresponding projected cross sections $\rho_{ij} d\sigma/dt$ in Figs. 2(f)–2(i). To leading order in $1/s$, $\rho_{00} d\sigma/dt$ and $\rho_+ d\sigma/dt$ ($\rho_- d\sigma/dt$) are, respectively, the cross sections for producing ω's of helicity 0 by unnatural parity exchange and of helicity 1 by natural (unnatural) parity ex-

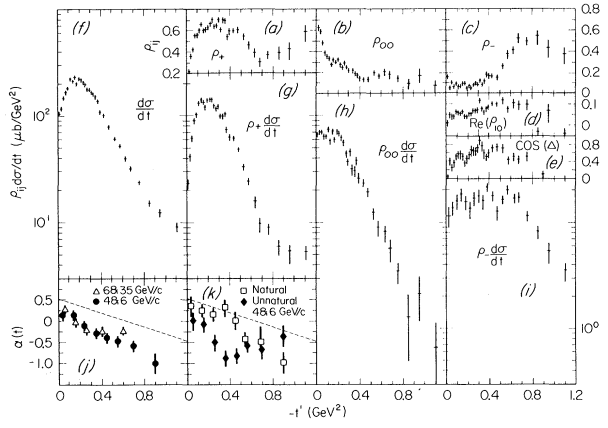

FIG. 2. (a)–(e) Density-matrix elements and coherence factor cosΔ in the s-channel helicity frame for $\pi^- p \to \omega^0 n$ versus t'. (f)–(i) Differential cross section and projected differential cross section versus t'. (j) Effective trajectory for $d\sigma/dt$, from our data and those of Ref. 3 (triangles) and of Ref. 1 (circles). (k) Effective trajectories for natural and unnatural parity exchange from our data and those of Ref. 1.

change. Coherence between unnatural-parity-exchange amplitudes for ω's with helicity 0 and 1 is measured by $\cos\Delta = \sqrt{2}\,\mathrm{Re}\rho_{10}/(\rho_{00}\rho_-)^{1/2}$ [Fig. 2(e)]. Rough information on the energy dependence has been obtained by combining our data with those from a $\pi^- p$ counter experiment[3] at an average momentum of 35 GeV/c, and from a 3500-event deuterium–bubble-chamber experiment[1] at 4 GeV/c. Figure 2(j) shows the effective trajectory $\alpha(t)$ for $d\sigma/dt$ (from $d\sigma/dt \propto P_{\mathrm{lab}}{}^{2\alpha-2}$); the points obtained from 6 and 35 GeV/c and those from 4 and 6 GeV/c are in satisfactory agreement. Separate trajectories for the natural- and unnatural-parity cross sections $\rho_+ d\sigma/dt$ and $(\rho_{00} + \rho_-) d\sigma/dt$ from the 4- and 6-GeV/c data are shown in Fig. 2(k). The ρ trajectory determined from $\pi^- p \to \pi^0 n$ is indicated for comparison by a dashed line.

Several features of the data deserve special comment:

(1) $\rho_{00} d\sigma/dt$ has no strong forward turnover, implying a sizable helicity-nonflip contribution. Unless absorption causes large helicity-mixing effects, this nonflip contribution cannot be accommodated[17,18] by models employing only ρ and B exchanges with the associated cuts. An alternative is to invoke the exchange of another unnatural-parity object "Z"[18] whose simplest quantum numbers would be $J^{PC} = 2^{-+}$. No experimentally observed particle has these quantum numbers.

(2) $\rho_+ d\sigma/dt$ shows a dramatic forward turnover of nearly an order of magnitude which is responsible for most of the turnover in $d\sigma/dt$. This is in pronounced contrast to the behavior of $\rho_+ d\sigma/dt$ in $\pi^- p \to \rho^0 n$, which shows a sharp forward peak usually attributed to absorptive effects (cuts); in a pure Regge-pole model $\rho_+ d\sigma/dt$ will vanish at $t = 0$. On the other hand $\rho_+ d\sigma/dt$ does not behave as if it is dominated at all t by ρ-pole exchange. There is only a suggestion of a dip near $|t| = 0.6$ (GeV/c)^2 where the ρ trajectory crosses zero. Also, the trajectory α_N for natural parity exchange lies increasingly below the accepted ρ trajectory at high $|t|$.

(3) The coherence factor cosΔ, which would be unity in simple B-pole exchange models, has a maximum near $t = -0.4$ (GeV/c)^2 and is small both near $t = 0$ and also at large $|t|$, implying spin and/or phase incoherence there.

(4) The effective trajectory α_U for unnatural parity exchange lies considerably below α_N in the vicinity of $t = -0.4$ (GeV/c)^2. Since this is also the region of maximum coherence it is perhaps the most reliable estimate of a point on the B trajectory. The small-t behavior of α_U is dominated by the "Z" effect.

We have profited greatly from conversations with A. C. Irving, R. D. Field, and A. B. Wicklund. We wish to thank H. Barton, P. Brockman, G. Hartner, R. Kammerud, D. Legacey, P. Patel, and C. Zanfino for their contribution to various phases of the experiment. We are indebted to J. Heimaster for software development, to H. Coombes, B. Dodge, J. Fitch, A. Kiang, and C. Rush for technical support, and to the staff of the zero-gradient synchrotron for efficient operation.

*Work supported in part by the U. S. Energy Research and Development Administration, The National Science Foundation, and the National Research Council of Canada.

†Present address: Physics Department, California Institute of Technology, Pasadena, Calif. 91125.

‡Present address: Department of Radiology, Stanford University, Stanford, Calif. 94305.

[1]M. N. Emms *et al.*, Rutherford Laboratory Report No. RL-75-067 (unpublished).

[2]W. D. Apel *et al.*, Phys. Lett. 55B, 111 (1975).

[3]V. N. Bolotov *et al.*, Phys. Lett. 53B, 217 (1974).

[4]J. C. Anderson *et al.*, Phys. Lett. 45B, 165 (1973).

[5]L. E. Holloway *et al.*, Phys. Rev. D 8, 2814 (1973).

[6]K. Paler *et al.*, Lett. Nuovo Cimento 4, 745 (1972).

[7]J. A. J. Matthews *et al.*, Phys. Rev. Lett. 26, 400 (1971).

[8]G. C. Benson *et al.*, Phys. Rev. Lett. 22, 1074 (1969).

[9]M. H. Shaevitz *et al.*, preceding Letter [Phys. Rev. Lett. 36, 5 (1976)].
[10]M. H. Shaevitz, Ph.D. thesis, The Ohio State University, 1975 (unpublished).
[11]V. Chaloupka *et al.*, Phys. Lett. 50B, 1 (1974).
[12]For more detail on the $M_{3\pi}$ region above the ω see N. R. Stanton, in Proceedings of the Argonne National Laboratory Summer Symposium "New Directions in Hadron Spectroscopy," Argonne, Illinois, 1975 (to be published).
[13]A comparable effect expected in the $\rho^0 N^{*0}$ charge state is suppressed by the experimental acceptance.
[14]G. Goldhaber, in *Experimental Meson Spectroscopy*, edited by C. Baltay and A. H. Rosenfield (Columbia Univ. Press, New York, 1970), p. 123.
[15]N. N. Achasov and G. N. Shestakov, Nucl. Phys. B45, 93 (1972).
[16]A. Rabl and N. W. Reay, Phys. Lett. 47B, 29 (1973).
[17]R. D. Field and D. P. Sidhu, Phys. Rev. D 10, 89 (1974); R. D. Field, private communication.
[18]A. C. Irving and C. Michael, Nucl. Phys. B82, 282 (1974).

Why Color Fails to Show in Electroproduction and Neutrino Scattering Experiments

Joseph C. Pati* and Abdus Salam†
International Centre for Theoretical Physics, Trieste, Italy
(Received 2 September 1975)

We show that the suppression of color-brightening effects in leptoproduction is a general property of a class of spontaneously broken color-gauge theories, based on integer-charge quarks.

(1) For gauge theories[1,2] based on integer-charge quarks, belonging for example to a $(\underline{4}, \underline{3}^*, \underline{1})$ representation of a symmetry group SU(4) $\otimes$ SU(3)$'\otimes$ U(1)$'$, electric charge has two components: $Q = Q_{\text{valency}} + Q_{\text{color}}$. A major dilemma for such theories is the experimental result from electroproduction experiments[3] that Q_{quark} is fractional and approximately equals Q_{valency}. There is little evidence for color to be produced on a par with valency. We shall refer to this experimental fact as lack of "color brightening." In this note we wish to show that the failure of color to brighten is a perfectly general property of all (spontaneously broken) gauge theories where (1) leptons are color singlets, and (2) valency and color are gauged independently, with weak interactions associated with valency gauging and strong with color gauging.

The argument is simple: Express the gauging pattern above symbolically in the form $L_{\text{int}} = gW_\mu(J_\mu^{\text{val}} + J_\mu^{\text{lep}}) + fV_\mu J_\mu^{\text{col}}$. Here W stands for the weak and V for the strong gauges, while the photon field A_μ is a mixture of W_3 and $\frac{1}{2}(\sqrt{3}V_3 + V_8)$. Notice now that before spontaneous symmetry breaking (when all fields are massless), leptons interact with the valency current through the intermediacy of W_μ's—*but there is no interaction between* J^{lep} *and* J^{col}. Because of spontaneous symmetry breaking, valency and color-gauge mesons mix. This generates (through diagonalization of fields) the massless color photon A_μ, but inevitably also the orthogonal color gauge partner $\tilde{U}_\mu$ (with mass m_U), both of which contribute to lepton-color interaction. The photon and the $\tilde{U}$ contributions would exactly cancel each other except for the difference in their propagators. It is on account of this *cancelation mechanism* that color brightening is suppressed and asymptotically integer-charge quarks behave as if they carried their fractional valency charges.

(2) *Valency and color gauging.*—Though the result stated in Sect. 1 is general, we present its derivation within the gauge model[2] $SU_L(2) \otimes SU_R(2) \otimes SU(4)'$. This has the advantage that the effects of spontaneous symmetry breaking and the resulting mass matrix are available in detail. The basic fermion multiplet is a hexadecaplet consisting of three quartets of red, yellow, and blue quarks and four leptons. The six gauges W_L, W_R, corresponding to $SU_L(2) \otimes SU_R(2)$, act on valency indices $[(u, d) + (c, s)]_{L,R}$ while fifteen gauges $V(\underline{15}) = V(\underline{8}) + X(\underline{3}) + X(\underline{3}^*) + S^0(\underline{1})$ correspond to local color symmetry SU(4)$'$. The reduction of $V(\underline{15})$ shown above is under the SU(3)$'$ subgroup of SU(4)$'$, which acts on the red, yellow, and blue quarks. [The leptons are singlets of this SU(3)$'$.] The gauge couplings associated with $W_{L,R}$ and V are $g_L^2/4\pi \simeq g_R^2/4\pi \simeq 2\alpha$ and $f^2/4\pi \approx 1$ to 10. Spontaneous symmetry breaking is introduced through Higgs-Kibble fields[2] to yield $m_{W_L^\pm} \approx 75$ GeV, $M_{W_R^\pm} \gtrsim 200$ GeV, and $m_X \sim m_S \approx 10^5$ GeV, while the SU(3)$'$ octet of color gluons $V(\underline{8}) = (V_\rho^\pm, V_{K^*}^\pm, V_3, V_8)$ acquire masses of the order of 3 to 5 GeV.

There are five neutral gauge fields $W_{3L,R}$,